

Defining the Characteristics of Active Spreading Centers

Catherine Wardell

University of Washington, School of Oceanography,

Box 355351, Seattle, Washington 98195

cwardell@uw.edu

5/2/2012

Non Technical Summary

The lithosphere is the rigid rock that comprises the shell of the earth and is formed from many tectonic plates that shift relative to each other. This shift occurs due to convection cells in the asthenosphere, the layer of viscous rock lying beneath the lithosphere; these cells are driven by heat transfer from the earth's interior to the earth's surface through molten rock. Where the molten rock is cycled up to the base of the lithosphere the heat is transferred to the lithosphere and the cooled molten rock of the asthenosphere diverges, creating friction with the overlying lithosphere and pulling the plates apart. This is known as a spreading center and is the point at which new oceanic crust is made. The rate at which the plates are spread has been determined as a major factor influencing topographical characteristics on the seafloor, affecting parameters such as surface roughness and axial morphology. The conducted research created a high resolution multibeam bathymetric survey of the Pacific-Rivera active spreading center by use of the EM 302 Multibeam Echosounder. Quantitative measurements of surficial geological features were determined for this area and then compared to bathymetric data available from the Endeavour Segment spreading center to determine characteristics common to all active spreading centers and those that occur only at specific spreading rates. This survey found that ridge elevation decreases with distance from the spreading center in common divergent boundaries; however, this occurrence can be affected by other parameters.

ABSTRACT

Spreading centers occur where tectonic plates are moving apart from each other creating new seafloor and mid-oceanic ridges. The rate at which the centers spread causes changes in the geological features of the seafloor. In this paper quantitative measurements of surficial geological features are calculated from a high resolution multibeam bathymetric survey of the Pacific-Rivera active spreading center and then compared to bathymetric data from the Endeavour Segment of the Juan de Fuca ridge to determine if the structural characteristics reflect their similarity in spreading rate. Common features such as progressive ridges were found at both locations, showing decreasing elevation with distance from the axial valley.

INTRODUCTION

The lithosphere is a layer of rigid rock that comprises the outermost shell of the earth and is comprised of many tectonic plates that shift relative to each other. This shifting occurs due to convection cells in the asthenosphere; these cells are driven by heat transfer from the earth's interior to the earth's surface through molten rock. As the heat reaches the base of the lithosphere it transfers to the lithosphere and the cooled molten rock of the asthenosphere travels out from the divergent plate boundary before cooling further and sinking back to the interior. The friction between the molten asthenosphere and the overlying lithosphere drives tectonic movement; this movement is not uniform throughout the lithosphere (Morgan, 1972; Davies, 2007).

Spreading rate has been shown to be a major factor influencing topographical characteristics at spreading centers, affecting parameters such as axial morphology and surface roughness. with many studies focusing upon features found only at specific spreading rates as well as those common to all spreading centers.

An axial volcanic ridge forms during a magmatic phase where there is intrusion of magma to the surface of the crust; this builds up until intrusion rates decrease. The plates diverge at this boundary due to new material forcing the plates apart but also due to pulling action experienced at corresponding edges of the oceanic plate as the plate subducts beneath continental crust at a continental margin. As magmatism declines the spreading pressure on the plate causes the new material to divide and subside to form a graben (Carbotte et al., 2006), leaving sharp scarps to either side which form the ridges. This process continues as the plates are pulled apart and the graben extends laterally to form an axial valley. If another intrusion event occurs then the new material contributes to the formation of a new axial volcanic ridge within the existing graben. This process repeats and so forms many ridges and valleys, which, once beyond the zone of intrusion impact become inactive. The distance between these ridges is dependent on periods of magmatic and tectonic activity and so may not necessarily show a trend.

There are three types of tectonic plate boundaries; 1) convergent, where plates are moving towards each other, 2) divergent, where they move apart or 3) transform, where motion is orthogonal to the plate boundary. Spreading centers occur at divergent plate boundaries where the molten rock convects upwards to the base of the lithosphere and diverges to the sides, causing the plates to move apart. Magma can erupt between the diverging plates as the

lithosphere is melted and forced upwards; this creates a mid-ocean ridge and new crust is formed from the erupted magma. As the plate moves away from the spreading center it cools by transfer of heat to the ocean, becoming denser and less buoyant while sinking relative to younger crust material (Ernst, 2000).

An example of a spreading center can be found extending from the Rivera triple junction (Faulds and Henry, 2008) where the Rivera, North American and Pacific Plates meet; the northern end of this Pacific-Rivera rise has a spreading rate of 50mm year^{-1} indicating that it is an intermediate spreading center (Demets and Stein, 1990). Another example of a spreading center is the Endeavour Segment of the Juan de Fuca ridge which also exhibits intermediate spreading rates of $56\text{-}57\text{mm year}^{-1}$ (Wilson, 1993; DeMets et al., 1994). Spreading rate has been determined as a major factor influencing topographical characteristics at spreading centers, affecting parameters such as surface roughness and axial morphology. The spreading rate also influences hazard extent and severity. An increase in spreading rate has been linked with a shallower axial valley and a decrease in roughness of the flanking topography (Ondréas et al. 2001; Small and Sandwell, 1992).

The spreading rate at the Pacific-Rivera rise is comparable to that at the Endeavour Segment and so common features such as surface roughness patterns and axial valley dimensions are anticipated. To test this assumption a high resolution multibeam survey was conducted across the Pacific-Rivera Rise and pattern metrics were calculated for the area. A comparison between the data collected and data from the Endeavour Segment has also been carried out in order to address whether the structural characteristics reflect the similarity in spreading rate. As the two

systems have similar spreading rates it is expected that the structural metrics on the surficial geological features will be alike, specifically;

- That the surface roughness patterns at the Pacific-Rivera Rise will closely resemble those at the Endeavour Segment.
- The seafloor elevation relative to the axial ridge will decrease with distance from the spreading center at each site.
- The axial valley characteristics, such as height and width will be similar.

A potential application for this research would be to assist in the development of a classification index for spreading centers that could be applied globally to allow inference of spreading mechanisms by observations of ridge morphology. If the quantitative patterns demonstrated at the spreading center match those only found at specific spreading rates then that site will share similar mechanisms as well, as the mechanisms are responsible for feature formation.

METHODS

Data acquisition

A 16 hour multibeam sounding survey was conducted in the area surrounding the Pacific-Rivera spreading center using the Kongsberg EM302 30 kHz multibeam echosounder. In this survey, data were collected on the RV Thomas G. Thompson from the 23 to the 24th March 2012 at depths ranging from 2400 to 3100m. The vessel speed was 6 knots and the beam angle was 65 degrees, although this was increased to 75 degrees in order to extend the reach of the multibeam sonar to account for a gap in the data. Sound velocity profiles were taken throughout the data

acquisition using a CTD at the beginning of the data acquisition and expendable bathythermograph (XBT) to account for variations in water column density that would affect the velocity of the sonar pulse.

Bathymetric data for the Endeavour Segment of the Juan de Fuca spreading ridge was acquired from the Visions'05 Hydrographic Survey (2005) (Figure 1).

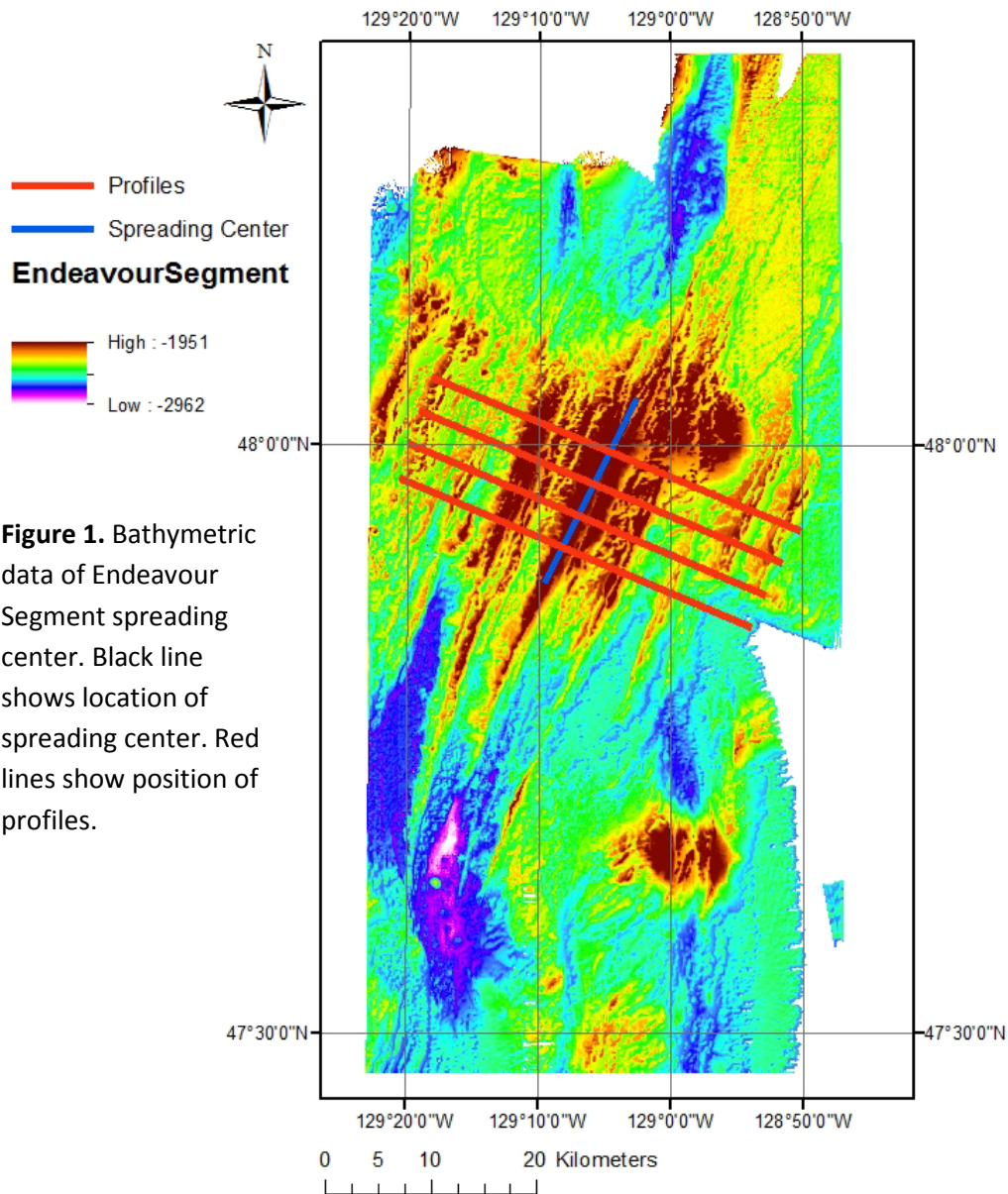


Figure 1. Bathymetric data of Endeavour Segment spreading center. Black line shows location of spreading center. Red lines show position of profiles.

Postprocessing

The survey track lines were imported to CARIS HIPS and SIPS where they were post processed to account for variations in sound velocity throughout the water column and movement of the vessel. Given that the average water depth (3000m) and the very low (<1m) variation in sea surface height due to tidal forcing, a zero-tide (no change) file was applied to all lines. Combined Uncertainty Bathymetric Estimator (CUBE) filtering was used to reject outlier soundings and then the subset editor was used to further clean the remaining outliers. The bathymetric data from the Endeavour Segment spreading ridge used for comparison was already processed at 30m resolution. In order to ensure accuracy in comparisons, related metrics were obtained from a 30m base surface (Figure 2).

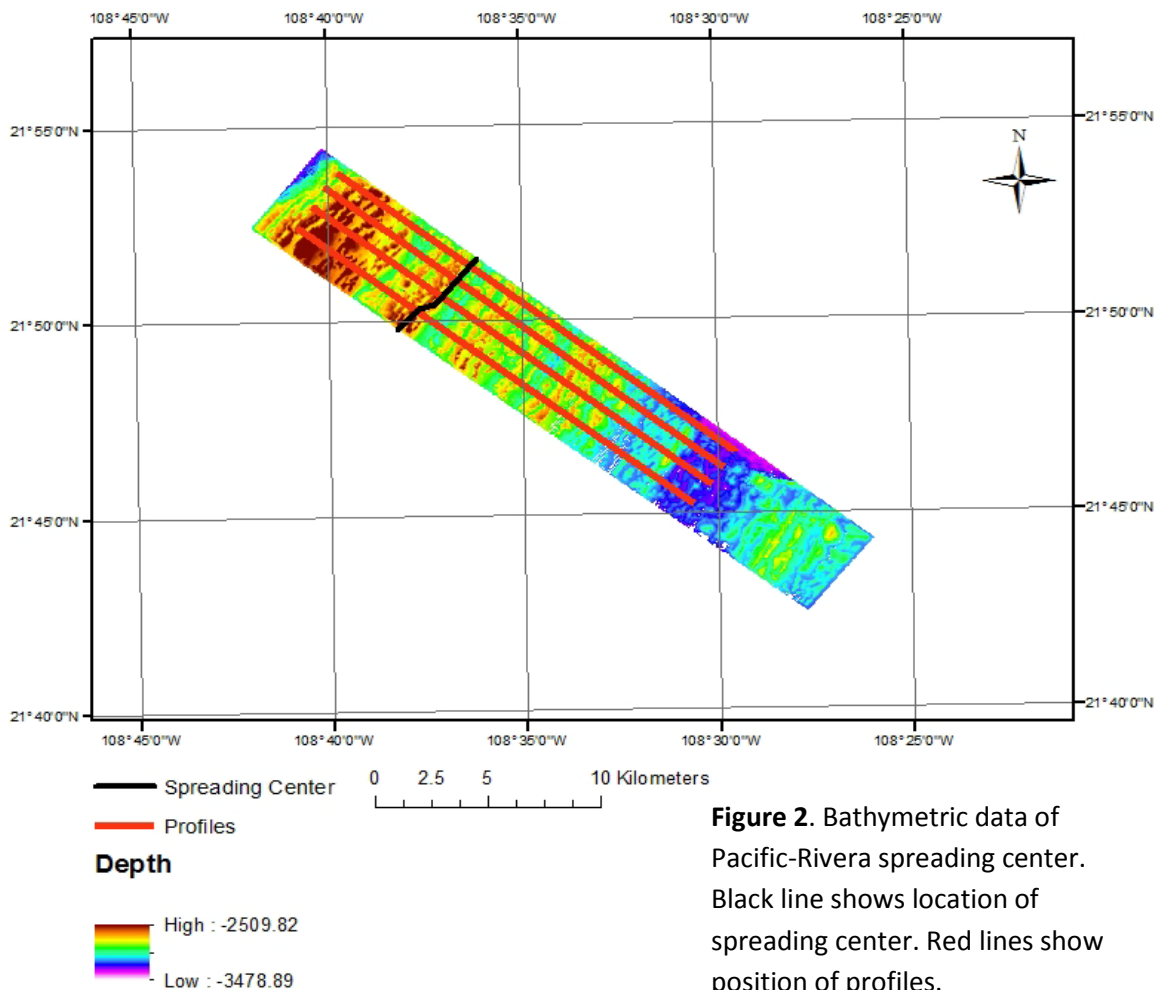


Figure 2. Bathymetric data of Pacific-Rivera spreading center. Black line shows location of spreading center. Red lines show position of profiles.

Pattern metrics

The base surfaces were exported to ESRI ArcGIS software for quantitative analysis alongside Endeavour Segment bathymetry data collected using the EM300 multibeam echosounder. The full extent of the survey included portions of an overlapping spreading center and transform fracture zone that were not part of my study, thus the final base surface was cropped to focus on the traditional spreading center in the south-western quadrant. Tectonic boundaries identified by Princeton University (Goodell, 2012) and the US Geological Survey using earthquake locations and magnetic anomalies were used alongside bathymetry base maps within ArcMap and study of the data to determine the spreading center axis.

Cross-sectional elevation transects were created at equally spaced intervals of approximately 1km at the Pacific-Rivera spreading center and 3km at the Endeavour Segment within ArcMap using the ArcGIS profile tool. This data was then exported to Microsoft EXCEL for the creation of profiles. Trendlines were applied to both the east and west of each spreading center in order to determine the elevation pattern of ridges with distance from the axial valley. Due to the larger extent of Endeavour Segment data it was possible to space the profiles further apart to analyze variation over a greater area. Axial valley height and width were determined within EXCEL. Height is defined as the mean distance from the highest point on opposing ridges to the lowest point found within the axial valley. Width, as defined by the distance between the highest points on opposing ridges on transecting profiles.

A directional buffer was created individually to both the east and west of the spreading center and applied as an analysis mask to allow calculation of spatial pattern statistics for both sides of the axial valley. A multiple ring buffer about each spreading center was created, at

1000m intervals to a distance of 15km (Figures 3 and 4). The area within each ring buffer for both separate directional masks was treated as an individual analysis zone for deriving descriptive statistics which characterize variation in the bathymetric surface of each zone.

Roughness of the landscape within each direction and zone was determined using the Jenness enterprises (Jenness 2005) surface area and ratio extension; this derives surface area using the variation of elevation in triangulation between the centerpoints of the central raster cell and those surrounding it. A ratio of this surface area to the planimetric area of the center raster cell is then calculated. The range in elevation as well as slope and its variation as a function of distance were calculated for each zone using ESRI Spatial Analyst toolset.

RESULTS

In all Pacific-Rivera profiles to the east of the spreading center, ridge elevation relative to the axial wall decreased with increasing distance from the axis; this trend becomes more pronounced while transitioning south (Figure 5). However, to the western extent of the survey the ridge elevation does not follow the aforementioned trend but increases with distance from the axis.

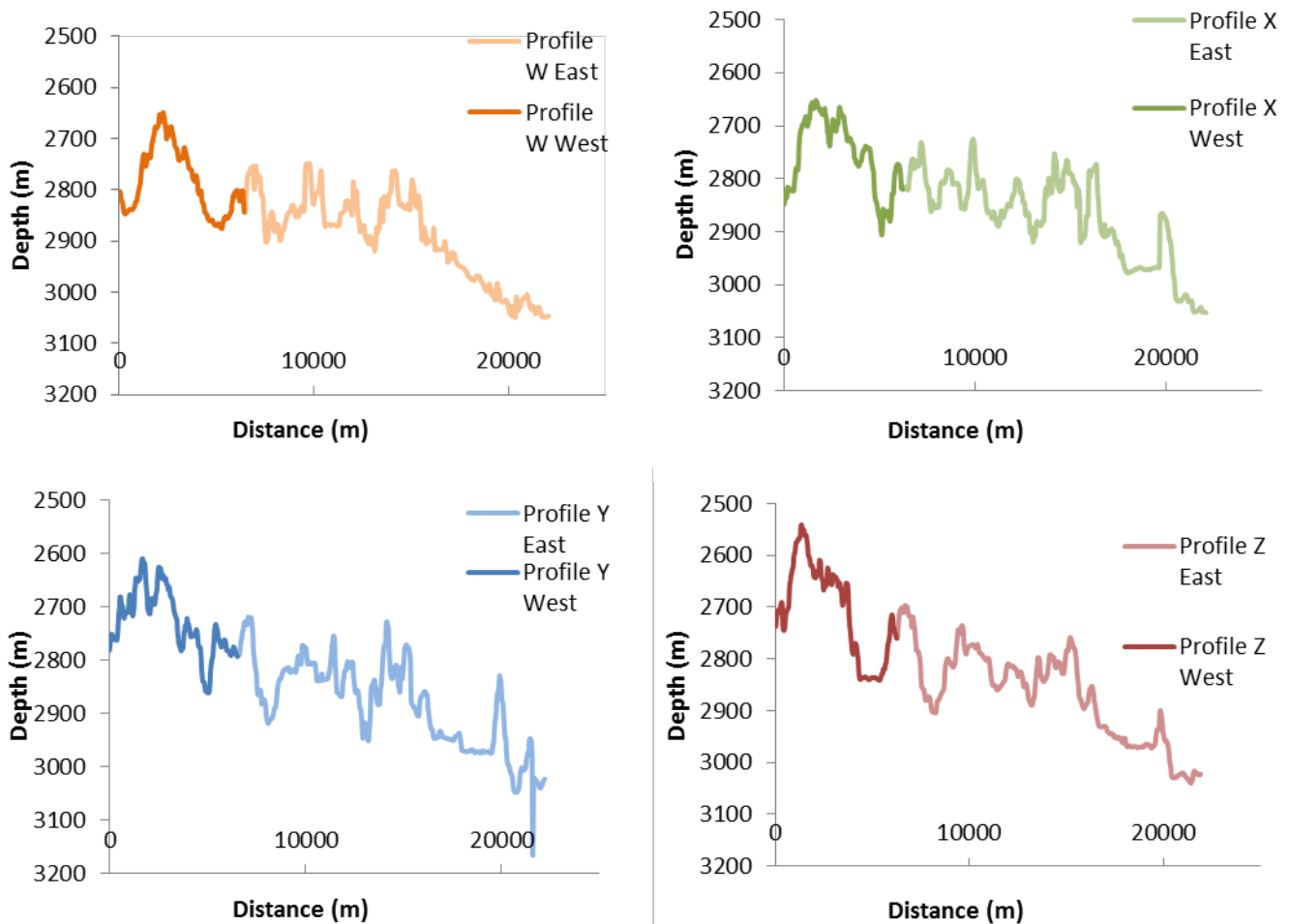


Figure 5. Profiles across the Pacific- Rivera spreading center showing the transition of the axial valley profile from the northern limit of the spreading center to the southern extent of the survey. Distance between profiles is approximately 1km.

The cross-sections of the Endeavour are distinctly more symmetrical than those at the Pacific-Rivera spreading center, with each side showing a decrease in ridge elevation with distance from the axial valley (Figure 6).

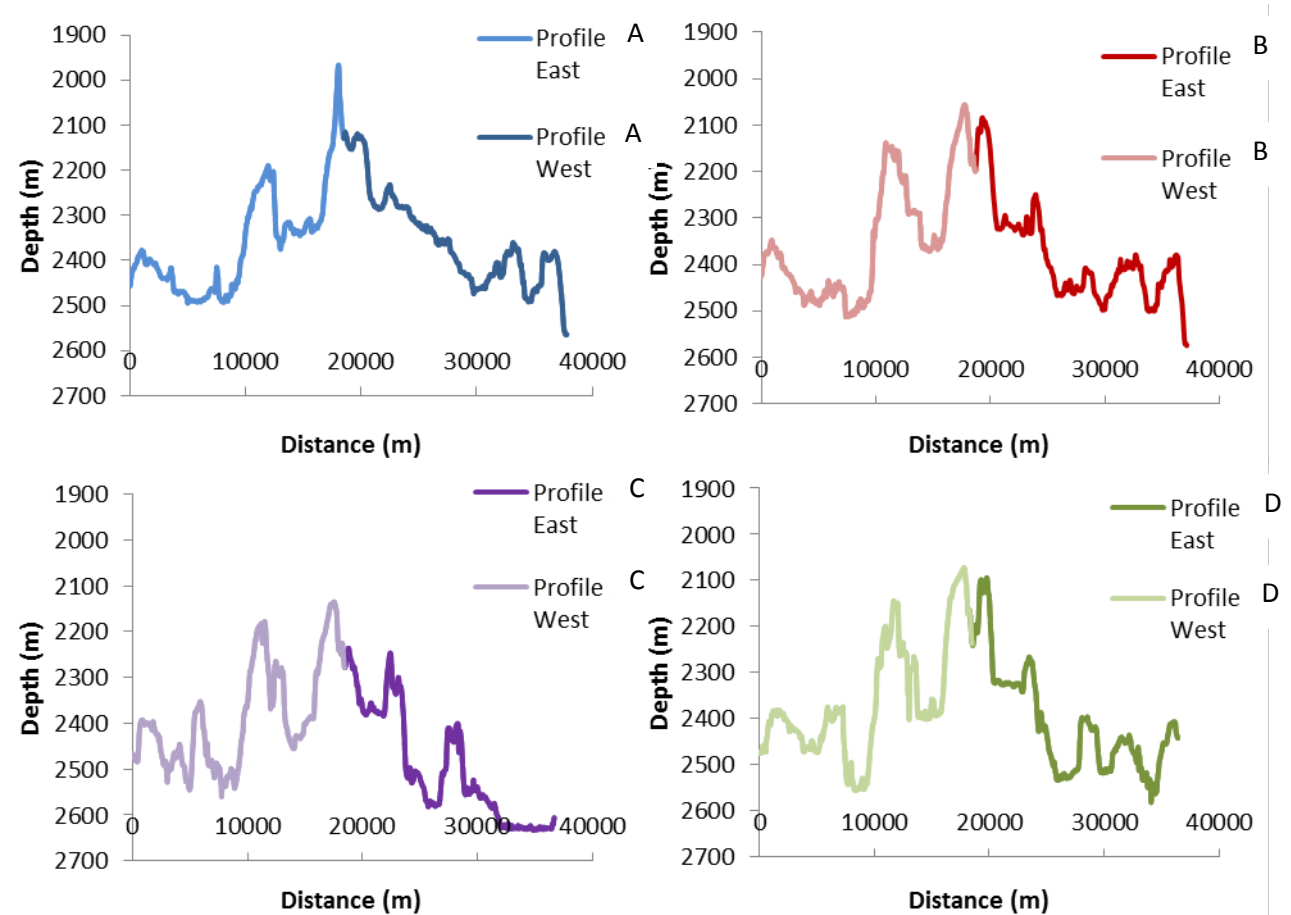


Figure 6. Profiles across the Endeavour Segment of the Juan de Fuca spreading center showing the transition of the axial valley profile from north to south. Distance between profiles is approximately 3km.

Profile	Height (m)	Width (m)
W	960	54.75
X	1228	61.25
Y	1500	68.50
Z	689	54.75

Table 1. Pacific-Rivera axial valley dimensions.

Profile	Height (m)	Width (m)
A	81.83	1374.51
B	117.98	1248.65
C	155.54	1500.34
D	35.24	2634.01

Table 2. Endeavour Segment axial valley dimensions.

Both spreading centers demonstrate similar axial valley patterns of increasing height while transitioning south before a final shallower range between the trench and crest of the axis. However, the height values at the Endeavour Segment are an order of magnitude larger than those at the Pacific-Rivera; the width measurements contrast this with the Pacific-Rivera having a much wider axial valley in comparison to the relatively narrow valley of the Endeavour Segment.

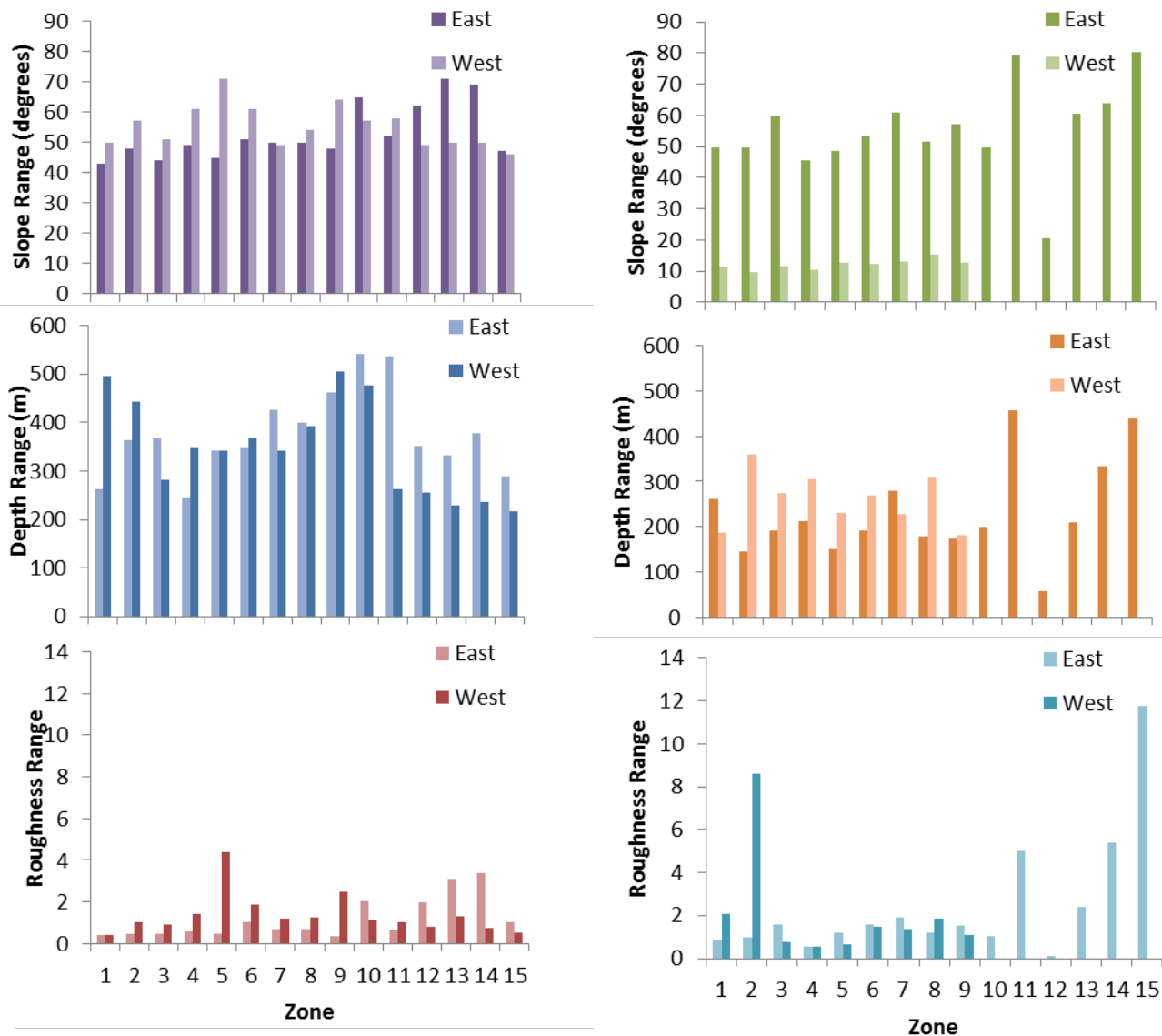


Figure 7. Zonal statistics from the Endeavour Segment spreading center (A, B, C) and the Pacific-Rivera spreading center (D, E, F). Each zone represents a 1000m interval extending 15km from the spreading center. A, D: Slope range for each zone to the East and West of the centers. B, E: Depth range. C, F: Roughness range.

The slope range, with the exception of the western area of the Pacific-Rivera spreading center, mostly varies within 40-60° and the slope variation to the east of each axis shows similar patterns with the largest variation at the outer limits of the survey (Figure 7). The roughness range also increases as a function of distance to the east of each survey, although the Pacific-Rivera (max 12) region shows variation on a much greater scale than that at the Endeavour Segment (max 4). The depth range of the Pacific-Rivera region demonstrates greater variability further from the center whilst each side of the Endeavour Segment show transitions between peaks and troughs.

DISCUSSION

The profiles from both the Pacific-Rivera spreading center and those at the Endeavour Segment show the presence of episodic ridges as well as an axial valley. Sonar surveys conducted by Kappel and Ryan (1986) confirmed the presence of an axial valley along the Juan de Fuca spreading ridge.

The elevation of the ridges decreases with distance from the axial valley, with the exception of some ridges at the north of the Pacific-Rivera spreading center and those to the west of it. The presence of the overlapping spreading center to the north of the survey area may have resulted in the compression of oceanic crust between the two axial volcanic ridges to form a larger ridge of higher elevation that otherwise may not have occurred. Therefore, the characteristics of the western side of the Rivera-Pacific ridge system shall not be considered as common to active spreading centers, although this phenomenon may be a common feature representative of overlapping spreading centers.

Newer magmatic material is of higher temperatures due to its close proximity to the axial magma chamber and so is buoyant and sits atop the underlying asthenosphere. However, as the material is transported beyond the zone of influence of the spreading center it is no longer heated by the underlying axial magma chamber and so the heat lost to the overlying water column is not replenished. This results in this older material becoming more dense and so sinking into the asthenosphere, therefore it is of lower elevation when compared to the newer material. LePichon and Langseth Jr (1970) found an almost linear relationship between slope and spreading rate, indicating that the spreading rate is linked to the heat flux to the water column. Potential application of this knowledge could help predict elevation of the seafloor where bathymetric data is not well collected but spreading rate has been estimated.

The creation of an index of characteristics for varying spreading rates would help with initial spreading center identification and possible hazard prediction. If an intermediate spreading rate demonstrates magma intrusion that causes the lithosphere to be elevated along the ridge then with increased magma intrusion at a fast spreading center it could be predicted that the ridge

would be of higher elevation and that due to the more rapid spreading rate the axial valley would be narrower. The reverse can be predicted at slow spreading centers. Further measurements and comparisons of varying spreading centers would be necessary to add to this index.

Conclusions

Sea floor topography is strongly influenced by spreading rate, with common features occurring to all active spreading centers as well as those of similar spreading rate. Spreading centers demonstrate axial volcanic ridges and, dependent on the tectonic and magmatic cycle can also have the presence of axial valleys. Ridges also extend from the spreading center and demonstrate a decrease in elevation with increasing distance; this phenomenon occurs regardless of spreading rate, although spreading rate can affect the overall elevation of the region. Further data compilation is necessary to form an index of active spreading center characteristics to allow prediction of conditions in area of little knowledge and potential applications of this to hazard mapping.

References

- Carbotte, S. M., R. S. Detrick, A. Harding, J. P. Canales, J. Babcock, G. Kent, E. Van Ark, M. Nedimovic and J. Diebold (2006) Rift topography linked to magmatism at the intermediate spreading Juan de Fuca Ridge. *Geology*. 34 (3) p209-212
- Davies, G.F. (2007). Whole mantle convection and plate tectonics. *Geophysical Journal of the Royal Astronomical Society*. 49 (2), p 459–486
- Demets, C. and S. Stein (1990). Present-day kinematics of the Rivera Plate and implications in southwestern Mexico. *Journal Geophysical Research*. 95 p 21931-21948
- DeMets, C., R. G. Gordon, D. F. Argus, and S. Stein (1994), Effect of recent revisions to the geomagnetic reversal timescale on estimates of current plate motions, *Geophys. Res. Lett.*, 21, 2191 – 2194.

- Ernst, W.G. (2000). *Earth systems: processes and issues*. Cambridge: Cambridge University Press. p87-88.
- Faulds, J. and C. Henry (2008). Tectonic influences on the spatial and temporal evolution of the Walker Lane: An incipient transform fault along the evolving Pacific – North American plate boundary. *Arizona Geological Society Digest* 22. 1 (1), p437-470.
- Goodell, L. (2012). *Using Google Earth to Explore Plate Tectonics*. Available: http://serc.carleton.edu/sp/library/google_earth/examples/49004.html. Last accessed 18th May 2012.
- Jenness, J. 2005. Random point generator (randpts.avx) extension for ArcView 3.x, v. 1.3. Jenness Enterprises. Available at: http://www.jennessent.com/arcview/random_points.htm.
- Kappel, E. S., W. B. F. Ryan. (1986) Volcanic Episodicity and a Non-Steady State Rift Valley Along Northeast Pacific Spreading Centers: Evidence from Sea MARC I. *Journal of Geophysical Research*. 91 (14) p13925-13940
- Keller, D.S., Embley, R., Lilley, M.D., Baross, J.A., Bemis, K., Butterfield, D., Chadwick, W., Cormier, M., Cowen, J., Delaney, R.R., Ding, K., Dziak, R., Feely, R., Johnson, H.P., Kadk, D., Lowell, R., Lupton, J., McDuff, R.E., Perfit, J., Resing W., Seyfried, D., Tivey, M.K., Tivey, M., Wilcock, W.D. Interaction of Crustal Evolution and the Biosphere at the Juan de Fuca Ridge. Accessed via: http://www.ridge2000.org/science/downloads/endeavour/endeavour_SiteProposal.pdf
Accessed on: 17/02/12
- LePichon, X. and M.G. Langseth Jr. (1969) Heat flow from the mid-ocean ridges and sea-floor spreading. *Tectonophysics*. 8 p 319-344
- Morgan, W.J. (1972). Deep Mantle Convection Plumes and Plate Motions. *AAPG Bulletin*. 56 (2), p. 203-213.
- Ondréas, H., D. Aslanian, L. Géli, J. Jean-Louis Olivet and A. Briais (2001). Variations in axial morphology, segmentation, and seafloor roughness along the Pacific-Antarctic Ridge between 56°S and 66°S. *Journal of Geophysical Research*. 106 (1), p8521-8543.
- Small, C. and D. Sandwell (1992). An Analysis of Ridge Axis Gravity Roughness and Spreading Rate. *Journal of Geophysical Research*. 97 (1), P3235-3245.
- Visions'05 Hydrographic Survey Technical Data Product (2005). 30m Bathymetric Gridded Data Endeavour Segment. University of Washington School of Oceanography. <http://www.ocean.washington.edu/>

Wilson, D. S. (1993), Confidence intervals for motion and deformation of the Juan de Fuca Plate, *J. Geophys. Res.*, 98, 16,053 – 16,071.

Yanchang, H. and P.D. Rabinowitz (1996). Spreading rate dependence of the axial topography and gravity of the Mid-Atlantic ridge between 22°N and 38°N. *Marine Geodesy*. 19 (3), p 215-233.